Available online at www.sciencedirect.com
ScienceDirect
Journal of Hazardous Materials 152 (2008) 1237–1247
Journal of Hazardous Materials
www.elsevier.com/locate/jhazmat

Analysis of CO_2 separation and simulation of a partially wetted hollow fiber membrane contactor

P. Keshavarz, J. Fathikalajahi *, S. Ayatollahi

Petroleum and Chemical Engineering Department, College of Engineering, Shiraz University, Shiraz, Iran

Received 23 April 2007; received in revised form 30 July 2007; accepted 31 July 2007
Available online 7 August 2007

Abstract

A steady state model was developed for a microporous hollow fiber membrane contactor operated under partially wetted conditions accompanied by chemical reactions, to analyze CO_2 absorption into the aqueous solution of diethanolamine (DEA). The proposed diffusion-reaction model contains reversible chemical reactions in the liquid bulk as well as wetted parts of the membrane pores. A numerical scheme was employed to solve the simultaneous nonlinear mathematical expressions, and the results were validated with experimental data in the literature. The gas phase concentration and velocity profile in axial direction inside the shell, liquid concentration profile in axial and radial directions inside the fibers, and also those within the wetted parts of the pores were predicted by using the model. The results of the model and proposed numerical scheme show that membrane wetting, even in very low fractions, can decrease the absorption flux significantly. The wetting fraction of membrane was predicted both with and without consideration of chemical reactions inside the wetted pores. The results indicate that the chemical reactions inside the wetted pores, which have been disregarded in the literature, have considerable effects on the prediction of membrane wetting fraction.

Keywords: Membrane contactor; Hollow fiber; Gas absorption; Partial wet

1. Introduction

Carbon dioxide is one of the major contributors to the greenhouse effect. There is an inexorable trend toward limiting anthropogenic emissions of carbon dioxide and other gases suspected of causing global climate change. Furthermore, the present interest in energy conservation and pollution control has led to search for more efficient and economical methods of CO_2 removal.

The application of microporous hollow fiber membrane contactor for gas absorption and stripping has gained considerable attention recently and still is a relatively new concept. In comparison with most membrane separation processes which use a dense selective layer on one side of the fibers, the microporous membrane used in membrane contactor is not selective. Instead of the selective layer, a liquid is flowed in one side of the fiber, which can absorb gas components physically or chemically. It leads to a higher mass transfer rate due to lower membrane resistance. Additionally, because there is no selective layer, a very small pressure drop across the membrane is required for mass exchange. Compared to the traditional columns like packed and tray towers, bubble columns, venture scrubbers and spray towers, membrane contactor has several advantages. These include higher mass transfer rates, independent control of gas and liquid rates, known and constant interfacial area, easy scale up and no operational problems such as foaming, flooding and entrainment [1,2]. By forming the membranes as hollow fibers, a very compact unit can be made with a specific area 1600–6500 ($m^2\,m^{-3}$), which is higher than 30–330 ($m^2\,m^{-3}$) offered by packed/tray towers and 160–500 ($m^2\,m^{-3}$) for mechanically agitated columns [1]. Although the membrane wall introduces an additional resistance, which does not exist in conventional towers, the higher surface area in this type of modules offers much higher mass transfer rates.

These advantages have led to a number of investigations on the use of membrane contactors for gas absorption and stripping. Absorption of various gases by a number of solvents in a hydrophobic membrane were first carried out by Zhang and Cussler [3,4]. Kreulen et al. [5,6] studied the CO_2 absorption

* Corresponding author.
E-mail address: zeglda@shirazu.ac.ir (J. Fathikalajahi).

0304-3894/$ – see front matter © 2007 Elsevier B.V. All rights reserved.
doi:10.1016/j.jhazmat.2007.07.115

Nomenclature

A_s	shell side cross-section area available for gas (m^2)
A_w	gas–liquid mass transfer area (m^2)
C	concentration (mol m^{-3})
C_g	total gas concentration (mol m^{-3})
C_{ig}	component gas concentration (mol m^{-3})
C_T	total amine concentration (mol m^{-3})
d_h	hydraulic diameter of shell side (m)
d_i	inner diameter of fiber (m)
d_O	outer diameter of fiber (m)
D	diffusivity (m^2 s^{-1})
D_{ik}	Knudsen diffusivity of species i (m^2 s^{-1})
H	Henry's constant
k_{-1}	reverse first order rate constant (s^{-1})
k_2	second order reaction rate constant (m^3 mol^{-1} s^{-1})
k_b	second order reaction rate constant for base b (m^3 mol^{-1} s^{-1})
K_{eq}	reaction (3) equilibrium constant (mol m^{-3})
K_{eq1}	reaction (7) equilibrium constant (mol m^{-3})
K_{eq2}	reaction (8) equilibrium constant
K_{ex}	external mass transfer coefficient (m s^{-1})
K_g	gas phase mass transfer coefficient (m s^{-1})
K_m	membrane mass transfer coefficient (m s^{-1})
L	module length (m)
M	molecular weight (kg $kmol^{-1}$)
P	pressure (Pa)
Q	volumetric flow rate (m^3 s^{-1})
r	radial direction or radius (m)
r_i	inner radius of fiber (m)
R	universal gas constant (J mol^{-1} K^{-1})
R_i	chemical reaction rate (mol^{-1} m^3 s^{-1})
Re	Reynolds number
Sc	Schmit number
Sh	Sherwood number
T	temperature (K)
U	velocity (m s^{-1})
x	wetting fraction
Z	axial coordinate (m)

Greek symbols

δ	membrane thickness
ε	membrane porosity
τ	tortuosity

Subscripts

A	carbon dioxide
B	amine
g	gas
i	any diffusing species
in	input
lm	log-mean average
L	liquid
p	pore
w	gas–liquid interface in the liquid filled pores

by water/glycol mixture as absorbent. Their results showed a better performance of membrane contactor compared to bubble column especially for higher viscous liquids. Karoor and Sirkar [7] studied absorption of CO_2 and SO_2 by water in a comprehensive experimental investigation and found that mass transfer rate is about ten times higher than those typically obtained in packed towers. Some other experimental and theoretical studies have been carried out focusing on CO_2 absorption from flue gases using various absorbents such as sodium hydroxide, potassium carbonate and alkanolamines [8–11]. The advantages of chemical absorption of CO_2 by alkanolamine or mixed alkanolamine solutions are quite obvious, since alkanolamines are weak basic compounds and their chemical bonds with CO_2 are easily broken at high temperatures, leading to efficient regeneration of the absorbents and as a result, can be recovered efficiently [12–16].

In most of these researches, hydrophobic membranes have been employed with gas filled membrane pores. In a hydrophilic fiber, pores are filled with a stagnant liquid film and mass transfer rate is much lower due to lower diffusivity of CO_2 in liquid. Therefore, the liquid phase pressure in a hydrophobic membrane should not exceed breakthrough pressure of the membrane to prevent membrane wetting. On the other hand, the pressure of liquid should be slightly higher than gas phase pressure to prevent dispersion of gas bubbles into the liquid.

Partial wetting can also occur when a hydrophobic membrane such as polypropylene (PP) or polyvinylidene florid (PVDF) is employed for gas absorption or stripping. Capillary condensation of water vapor in the pores, as well as pressure difference between shell side and lumen side, can be possible reasons for partial wetting [17,18]. The presence of organic compounds in the liquid phase, such as amine solutions, can decrease the surface tension of liquid and cause partial wetting. Some inorganic species, complexes, microorganisms or even traces of impurities can have the same effects [19,20]. Mahmud et al. [17,18] and Evren [21] studied the stripping of air from water and stated that the theory and experiments do not agree well in some cases. They attributed this disagreement to the partial wetting and a good fit was searched by changing the wetting fraction in the model. Such disparity between theory and experimental results has also been observed when a chemical reaction occurs in the liquid phase [22–24]. In the recent case, the partial wetting has been assumed again, but the same procedure of Mahmud et al. [17] was applied to search the wetting fraction, without consideration of chemical reaction in the liquid filled pores.

Some researchers try to overcome membrane wetting by using new absorbents or new membrane types. Kumar et al. [25] proposed a new chemical absorbent based on amino acid salts for CO_2 absorption with no wetting effect on polyolefin fibers. Recently, Yan et al. [26] employed aqueous potassium glycinate solution, which has the same influence. deMontigny et al. [27] compared the performance of polypropylene and polytetrafluoroethylene (PTFE) fibers using amine solutions and found that polypropylene membranes suffer a loss in performance over time, while PTFE membranes maintain their initial level of performance. It was attributed to the higher wetting resistance of PTFE compare to PP in amine solutions.

The previous investigations show clearly that the partial wetting phenomena can decrease mass transfer rate of hydrophobic membranes significantly, which is one of the most significant challenges in the long term application of membrane contactors. Therefore, more detailed theoretical and experimental investigations are required for better understanding of the partially wetted operating conditions.

In this paper, a theoretical analysis was performed for microporous hollow fiber membrane modules employed for CO_2 absorption, from a CO_2–N_2 gas mixture into the aqueous solution of diethanolamine (DEA), operated under partially wetted conditions. Governing equations for the gas phase within the shell side, the liquid phase within the lumen side and the liquid filled pores of the module were developed. For both the liquid bulk and wetted parts of the membrane pores, the diffusion-reaction model is based on reversible chemical reactions instead of a simple forward reaction rate model which has been previously used in the literature. A numerical scheme was proposed to solve the simultaneous nonlinear mathematical expressions and the results were validated with experimental data of Wang et al. [14]. The wetting fraction of membrane was searched for short time and long time running of the module and by considering the effect of chemical reaction inside the wetted parts of the pores, the effect which has been neglected in previous investigations.

2. Model description

A mathematical model is developed here to describe CO_2 absorption from a gas mixture using DEA aqueous solution. In all parts of this study, liquid is assumed to flow inside the fibers and countercurrent to gas flow inside the shell. Figs. 1 and 2 illustrate the mass transfer regimes in a single fiber. Gaseous component "*i*" can diffuse from the shell side to the membrane wall, passes through the gas filled and then liquid filled parts of the pores, and finally followed by liquid phase diffusion/chemical reaction. The following assumptions were made in deriving the mathematical expressions:

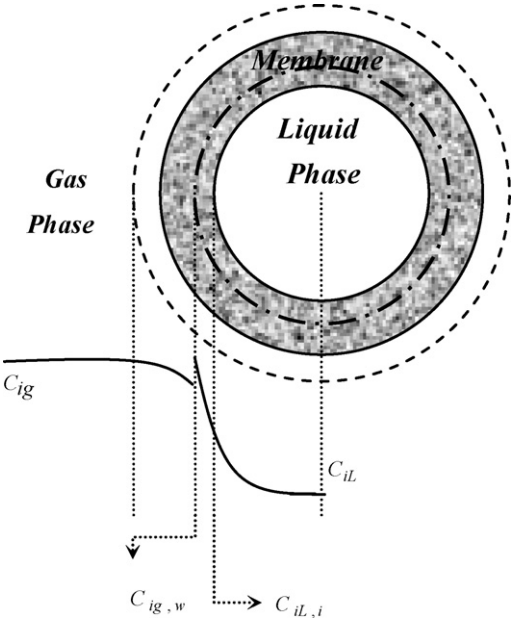

Fig. 1. Mass transfer regimes in a single fiber.

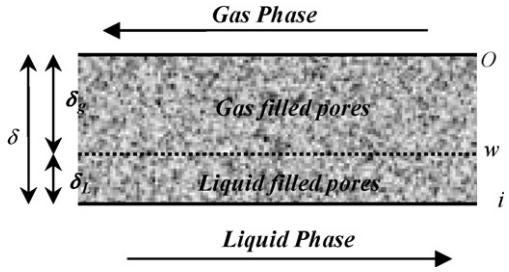

Fig. 2. Membrane wall sections under partial wet condition.

- Steady state and isothermal conditions.
- Laminar parabolic velocity profile within the fibers.
- Ideal gas behavior.
- No axial mixing in phases.
- Uniform pore size distribution and membrane wall thickness.

Using the above assumptions, the mathematical formulation of the liquid, gas and membrane phases are given as follows.

2.1. Chemical reactions

Mass transfer can be enhanced when a chemical reaction is present and it is usually unavoidable for a high recovery gas absorption process. The reaction of carbon dioxide with primary and secondary amines can be expressed by zwitterions mechanism as initially proposed by Caplow [28] and followed by Dankverts [29]. The first step is production of an intermediate zwitterion as follows [30–32]:

$$CO_2 + RR'NH \underset{k_{-1}}{\overset{k_2}{\longleftrightarrow}} RR'NH^+COO^- \quad (1)$$

Theoretically, the zwitterion can be deprotonated by any base present in the solution producing a carbamate ion and a protonated base:

$$RR'NH^+COO^- + B \overset{k_b}{\longleftrightarrow} RR'NCOO^- + BH^+ \quad (2)$$

Then, the overall chemical reaction of DEA with CO_2 is given by:

$$CO_2 + 2RR'NH \leftrightarrow RR'NCOO^- + RR'NH_2{}^+ \quad (3)$$

Glasscock et al. [32] introduced reversibility into this mechanism which necessarily be included for one to describe both absorption and desorption conditions. Rinker et al. [33,34] proposed a rate model by considering all possible chemical reactions in reversible form. According to that model and based on the assumption of quasi-steady state for the zwitterion, we have:

$$R_{CO_2} = \frac{k_2}{1 + (k_{-1}/K_{DEA}[RR'NH])} \times \left([CO_2][RR'NH] - \frac{[RR'NH_2{}^+][RR'NCOO^-]}{K_{eq}[RR'NH]}\right) \quad (4)$$

Table 1
Physical and chemical properties used in this study at 298 K [26,28,29]

D_{CO_2} ($m^2\ s^{-1}$)	D_{DEA} ($m^2\ s^{-1}$)	H	k_2 ($m^3\ mol^{-1}\ s^{-1}$)	k_{-1}/k_{DEA} ($mol\ m^{-3}$)	K_{eq} ($m^3\ mol^{-1}$)	K_{eq1} ($m^3\ mol^{-1}$)	K_{eq2}
$1.046E^{-9}$	$4.967E^{-10}$	0.76	4.089	3602.6	2.902	0.0091	0.036

$$R_{DEA} = \frac{2k_2}{1 + (k_{-1}/K_{DEA}[RR'NH])} \times \left([CO_2][RR'NH] - \frac{[RR'NH_2^+][RR'NCOO^-]}{K_{eq}[RR'NH]}\right) \quad (5)$$

Under steady state condition, the assumption of equal diffusivity of all amine species leads to:

$$C_T = [RR'NH] + [RR'NH_2^+] + [RR'NCOO^-] \quad (6)$$

An equilibrium model based on the model given by Astarita et al. [35] is used here to consider the distribution of bicarbonate and carbonate ion concentrations, with the assumption of the following equilibrium reactions:

$$RR'NH + HCO_3^- \overset{K_{eq1}}{\longleftrightarrow} RR'NCOO^- + H_2O \quad (7)$$

$$RR'NH + HCO_3^- \overset{K_{eq2}}{\longleftrightarrow} RR'NH_2^+ + CO_3^{2-} \quad (8)$$

The combination of electronutrality of ionic species and Eq. (6), as well as equilibrium relations of reactions (7) and (8), leads to the following equation:

$$\frac{2K_{eq2}}{K_{eq1}} \frac{[RR'NCOO^-]}{C_T - [RR'NH] - [RR'NCOO^-]} + \left(\frac{1}{K_{eq1}[RR'NH]} + 2\right)[RR'NCOO^-] + [RR'NH] - C_T = 0 \quad (9)$$

Here, carbamate concentration is a function of amine concentration and total amine molarity. Eq. (9) has been written in such a format proper to the solution algorithm given later in Section 3. The carbamate concentration is calculated with the known amine concentration by using Eq. (9), and the other ionic concentrations can be evaluated from Eqs. (6)–(8).

The values of required physicochemical properties are listed in Table 1.

2.2. Governing equations in liquid phase

The mass transfer phases for gas absorption in a hollow fiber membrane contactor under countercurrent condition and partially wetted mode are shown in Fig. 2. Applying a component material balance on the liquid phase within the fibers for *i*th diffusing component, leads to the following two-dimensional partial differential equation:

$$U_z \frac{\partial C_{iL}}{\partial Z} = D_{iL}\left(\frac{\partial^2 C_{iL}}{\partial r^2} + \frac{1}{r}\frac{\partial C_{iL}}{\partial r}\right) - R_i, \quad 0 \le r \le r_i \quad (10)$$

where R_i is the rate of chemical reaction for component i. The liquid flow rate inside the fiber is laminar and can be given by:

$$U_z = 2U_{av}\left[1 - \left(\frac{r}{r_i}\right)^2\right] \quad (11)$$

Eq. (10) consists of a set of partial differential equation, which should be written for all necessary components in the liquid phase. Since the chemical reaction term (R_i) is normally a function of concentration of several components, the partial differential equations are not independent and must be solved simultaneously. The initial condition for each diffusing component in the lumen is specified as:

$$C_{iL} = C_{iL,in}, \quad \text{for } Z = 0 \text{ and } 0 \le r \le r_i \quad (12)$$

At the center of each fiber, symmetry is assumed in radial direction, which results the following boundary condition:

$$\frac{\partial C_{iL}}{\partial r} = 0, \quad \text{for } r = 0 \text{ and all } Z \quad (13)$$

In the partial wetted mode, additional equations are required to describe diffusion-reaction inside the wetted parts of the pores. At high porosity (greater than 10%), the diffusion process is essentially one-dimensional as it has been shown by Keller and Stein [36]. Therefore in the liquid filled part of the pores we have:

$$D_{iL_e}\left(\frac{\partial^2 C_{iL}}{\partial r^2} + \frac{1}{r}\frac{\partial C_{iL}}{\partial r}\right) - R_i = 0, \quad r_i \le r \le r_w \quad (14)$$

D_{iL_e} is the effective diffusivity of diffusing species within the wetted pores and can be define as:

$$D_{iL_e} = \frac{D_{iL}\varepsilon}{\tau} \quad (15)$$

At the membrane–liquid bulk interface, the mass conservation leads to the following boundary condition:

$$D_{iL}\frac{\partial C_{iL}}{\partial r} = D_{iL_e}\frac{\partial C_{iL}}{\partial r}, \quad \text{for } r = r_i \text{ and all } Z \quad (16)$$

At the gas–liquid interface, a mass conservation for each diffusing species leads to:

$$D_{iL_e}\frac{\partial C_{iL}}{\partial r} = K_{ex}(C_{ig} - C_{ig,w}), \quad \text{for } r = r_w \text{ and all } Z \quad (17)$$

Also, Henry"s law can be applied at the gas–liquid interface as follows:

$$C_{iL} = HC_{ig}, \quad \text{for } r = r_w \text{ and all } Z \quad (18)$$

External mass transfer coefficient (K_{ex}) is a combination of gas filled parts of the membrane and shell side mass transfer coefficient and will be discussed in detail later. For some species in

liquid phase which cannot diffuse to gas, such as diethanolamine, Eq. (17) can be simplified as:

$$-D_{iL_e}\frac{\partial C_{iL}}{\partial r}=0,\quad \text{for } r=r_w \text{ and all } Z \tag{19}$$

It should be noted that a nonwet system is a special case of partial wet mode where $r_w = r_i$ and $D_{iL_e} = D_{iL}$.

2.3. Governing equations in gas phase

Eq. (17) indicates that the liquid phase concentration profile in the wetted pores and inside the fibers depend on the gas phase concentration distribution inside the shell. If the gas in the shell side is assumed to be pure or nearly pure, the assumption that is used frequently in previous researches [12,20,21,37], it is possible to use a constant gas concentration in Eq. (17), which leads to more simple problem. However, in practical applications of membrane contactor for gas absorption, for example in flue gas treating or gas sweetening, gas phase is a mixture of several components and therefore, gas phase conservation distribution must be considered.

By applying a component mass concentration on gas phase for each diffusing components, the following ordinary differential equation is proposed:

$$\frac{d}{dZ}(U_g C_{ig})-\frac{A_w}{A_s L}K_{ex}(C_{ig}-C_{ig,w})=0 \tag{20}$$

where A_w and A_s are the gas–liquid mass transfer area and shell side cross-section area available for gas, respectively. An overall mass balance for gas phase also gives:

$$\frac{d}{dZ}(U_g)-\frac{A_w}{A_s C_g L}K_{ex}(C_{ig}-C_{ig,w})=0 \tag{21}$$

The following boundary conditions can be employed for these equations:

$$C_g=\frac{P_g}{RT},\quad \text{at } Z=L \tag{22}$$

$$U_g=\frac{Q_g}{A_s},\quad \text{at } Z=L \tag{23}$$

When a gas mixture is analyzed, the sets of Eqs. (10)–(23) should be solved simultaneously for all diffusing components.

2.4. External mass transfer coefficients

The external mass transfer coefficient (K_{ex}) used in previous equations, is a combination of membrane wall and gas phase mass transfer coefficients. Application of resistance-in-series model for these two phases gives:

$$\frac{1}{K_{ex}d_i}=\frac{1}{K_g d_o}+\frac{1}{K_m d_{lm}} \tag{24}$$

Under partial wet condition, membrane mass transfer coefficient consists of two different parts: gas filled and liquid filled. Rangwala [22] and Mahmud et al. [17] combined the resistances of these two parts according to the following equation:

$$\frac{1}{K_m d_{lm}}=\frac{\tau\delta(1-x)}{D_{ig_e}\varepsilon d_{lm_g}}+\frac{\tau\delta x}{D_{iL}\varepsilon d_{lm_L}H} \tag{25}$$

d_{lm_L} and d_{lm_g} are the log-mean diameter of liquid filled and gas filled parts of membrane, respectively. Membrane wetting fraction (x) is the fraction of liquid filled pores and can be defined as (Fig. 2):

$$x=\frac{\delta_L}{\delta} \tag{26}$$

It should be emphasize that Eq. (25) has been derived with the assumption of no chemical reaction inside the wetted pores. Therefore, the external mass transfer coefficient which results from Eqs. (24) and (25) is the representative of gas phase in shell and both gas filled and liquid filled membrane resistances.

In presence of a chemical reaction inside the liquid filled pores, the combination of resistances are not simple. The method which is proposed here is the combination of gas phase resistance in the shell side and gas filled membrane resistance in the following form:

$$\frac{1}{K_{ex}d_i}=\frac{1}{K_g d_o}+\frac{\tau\delta(1-x)}{D_{ig_e}\varepsilon d_{lm_g}} \tag{27}$$

Subsequently, the relations for the liquid filled pores accompanied by chemical reaction will be covered by Eqs. (14)–(16).

Because of very small pore size, the gas diffusion in the gas filled pores is affected by pore wall, and Knudsen diffusion must be considered.

$$\frac{1}{D_{ig_e}}=\frac{1}{D_{ik}}+\frac{1}{D_{ig}} \tag{28}$$

Knudsen diffusion coefficient can be written as [38]:

$$D_{ik}=\frac{d_p}{3}\left(\frac{8RT}{\pi M}\right)^{1/2} \tag{29}$$

The gas phase mass transfer coefficient (K_g) should be evaluated from empirical correlations. Yang and Cussler [39] proposed the following correlation to estimate shell side mass transfer coefficient for axial flow in the hollow fiber modules:

$$Sh=1.25\left(Re\frac{d_h}{l}\right)^{0.93}Sc^{0.33} \tag{30}$$

Table 2 shows the specifications of hollow fiber module which has been modeled in this study.

3. Method of solution

The set of Eqs. (10)–(23) includes a number of partial and ordinary differential equations of first and second order. The partial differential equations are nonlinear, because of chemical reaction terms and must be solved simultaneously to find liquid concentration profile in radial and axial directions, and gas concentration/velocity profile in axial direction. Because of mathematical complexity of the proposed system, a numerical

Table 2
Specifications of hollow fiber membrane module [14]

Fiber o.d. (μm)	Fiber i.d. (μm)	Module length (cm)	Number of fibers	Porosity (%)	Tortuosity	Pore size (μm)
300	220	11.3	1100	40	3.5	0.04

technique should be applied to solve the equations. A finite difference scheme was employed to solve the equations by using MATLAB [40]. The diffusion terms were discretized implicitly, which generated sets of simultaneous nonlinear algebratic equations. We have found that Newton's method did not converge, especially when wetting fraction is high, because of highly nonlinearity of chemical reaction term. We, therefore, rewrote the chemical reaction term based on this fact that the amine concentration does not have sharp variation in axial direction as follows:

$$\frac{k_2}{1+(k_{-1}/K_{\mathrm{DEA}}[\mathrm{RR'NH}]_{j+1,i+1})}\left([\mathrm{CO_2}]_{j+1,i+1}\left[\mathrm{RR'NH}\right]_{j+1,i+1}-\frac{[\mathrm{RR'NH_2}^+]_{j+1,i+1}[\mathrm{RR'NCOO}^-]_{j+1,i+1}}{K_{eq}[\mathrm{RR'NH}]_{j+1,i+1}}\right)$$
$$\approx \frac{k_2}{1+(k_{-1}/K_{\mathrm{DEA}}[\mathrm{RR'NH}]_{j+1,i})}\left([\mathrm{CO_2}]_{j+1,i+1}[\mathrm{RR'NH}]_{j+1,i}-\frac{[\mathrm{RR'NH_2}^+]_{j+1,i}[\mathrm{RR'NCOO}^-]_{j+1,i}}{K_{\mathrm{eq}}[\mathrm{RR'NH}]_{j+1,i}}\right) \quad (31)$$

here j and i are the indications of radial and axial increments, respectively. It should be noted that CO_2 concentration was put as unique unknown term in the right hand side of Eq. (31) due to its wide change in axial direction. Using Eq. (31) and as an initial guess, a set of simultaneous linearized algebratic equations in radial direction were produced, which formed a tridiagonal matrix and were solved simultaneously using Thomas algorithm [41].

The amine concentrations produced from this initial guess were used in Eqs. (6)–(9) to find other ion species and the solution procedure was continued till convergence was attained. To prevent divergence, relaxation was used on the concentrations of amine and amine ionic species to stabilize the iterative solution process.

Because the governing equation in gas and liquid phases cannot be solved separately, a value for $(C_{ig} - C_{ig,w})$ was assumed at the beginning. This value should be adjusted according to the solution algorithm for the system, which is given schematically in Fig. 3. A material balance error was evaluated at the end of the program to check the accuracy of numerical technique. The average error is something around ±0.05% which is essentially acceptable for a finite difference method.

4. Results and discussion

The results of numerical study carried out with the proposed algorithm are presented below for the countercurrent flow pattern. The liquid inlet part of the module selected as zero ($Z=0$) in axial direction for all parts of this study. The analysis of model results and the comparison with experimental data of Wang et al. [14] has been done in two different conditions. These include short term analysis and long term analysis as follows.

4.1. Short term analysis

This part refers to the initial step of module operation, a while after module start up when wetting fraction is still low and for a short period of time the absorption flux is relatively constant [20]. It should be emphasize that the partial wetting of membrane can even occur in this initial step, because as a routine rule, an experimental apparatus should operate for at least half an hour before any data collection, to ensure that a steady state condition has been achieved.

The CO_2 absorption flux and absorption recovery obtained from the model and experimental results of Wang et al. [14] are shown in Fig. 4 with the assumption of no membrane wetting ($x=0\%$). The figure indicates that although there is a good agreement between model and experiment in low gas flow rates, the model prediction is much higher in high gas rates. Such result is similar to some other chemical and physical investigations in the literature [17–23].

Fig. 5 presents the model results with the assumption that membrane is partially wet. It is indicated from the figure that by employing a very small wetting fraction, $x=0.4\%$, a very good agreement between model and experiment can be obtained for all range of gas flow rates. It should be noted that the effects of chemical reaction inside the wetted pores, which was ignored in previous investigations [22–24], has been considered in the simulation results shown in this figure. Fig. 5 also reveals that the CO_2 recovery decreases with the increase of gas velocity, which is due to the reduction of liquid/gas ratio in the module.

To check the importance of chemical reaction inside the liquid filled pores in the prediction of wetting fraction, the model was run again under partially wetted condition, but with the assumption of no reaction within the liquid filled pores. In such a case, Eqs. (24) and (25) were employed instead of Eqs. (14)–(16) and (27), and the results are shown in Fig. 6. The wetting fraction used here is $x=0.25\%$, which is smaller but close to 0.4% employed in Fig. 5. The recovery and flux at $x=0.4\%$, without consideration of reaction in pores, are also shown in this figure for comparison. The figure reveals that the difference between simulation results at $x=0.25$ and 0.4% and both with experimental results are low, especially in low gas rates. The comparison of searched wetting fractions in Figs. 5 and 6 under short time operating conditions reveals that the consideration of chemical

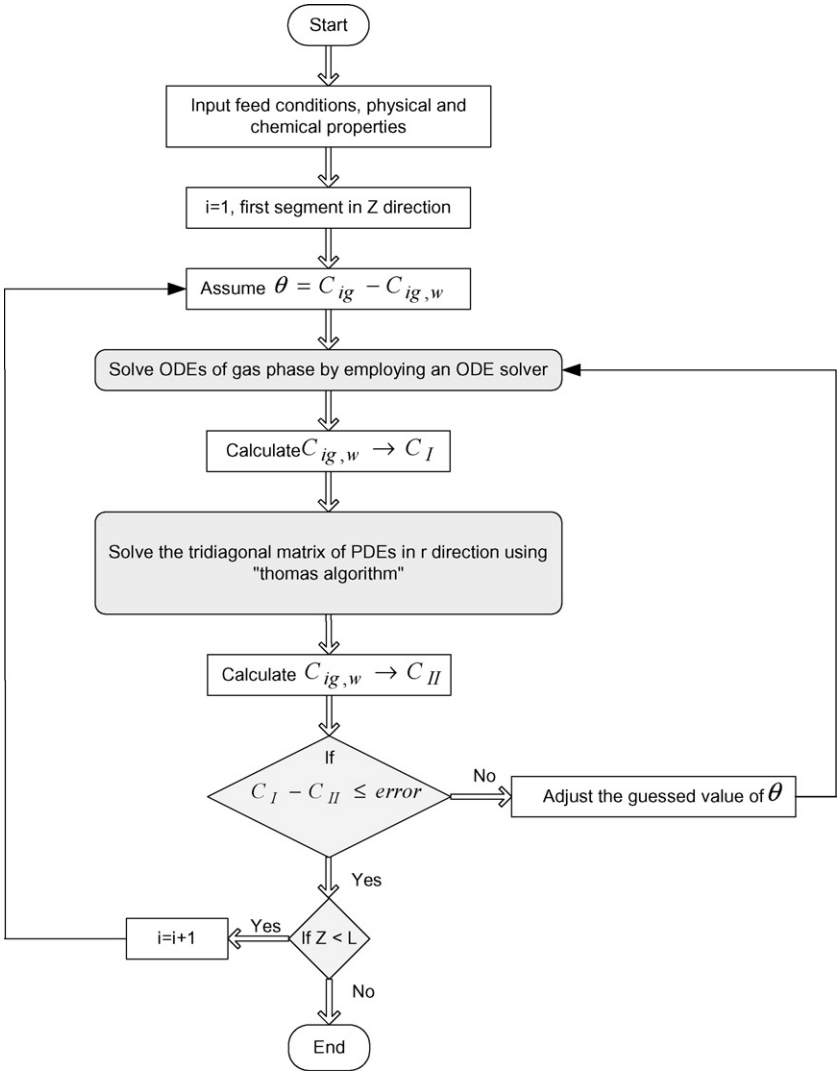

Fig. 3. Solution algorithm of the model.

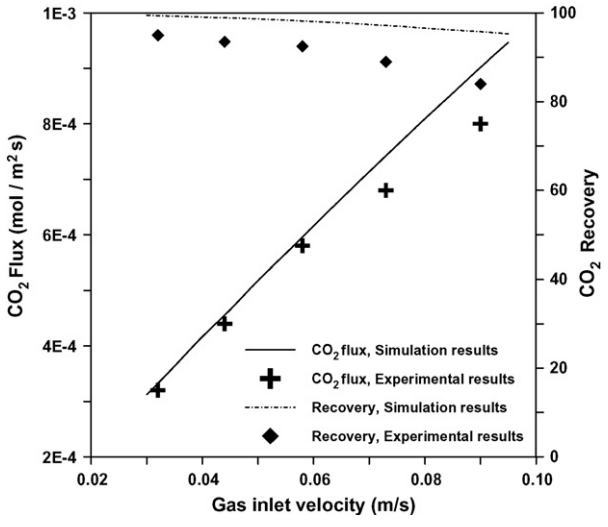

Fig. 4. CO_2 absorption flux and CO_2 recovery from a 20% CO_2–N_2 gas mixture under nonwet condition, $U_L = 0.12$ (m s^{-1}), $x = 0$.

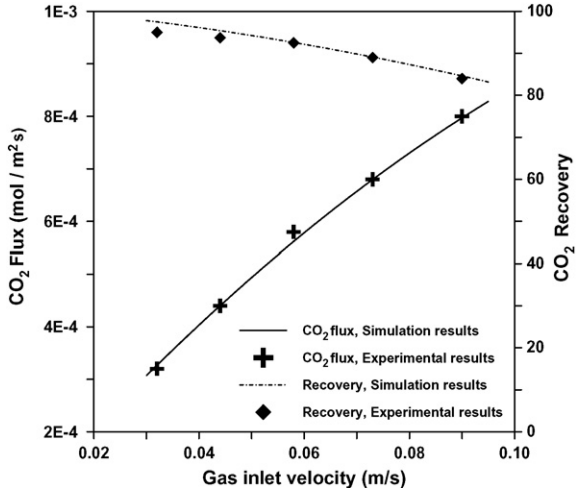

Fig. 5. CO_2 absorption flux and CO_2 recovery from a 20% CO_2–N_2 gas mixture with consideration of reactions in the liquid filled pores, $U_L = 0.12$ (m s^{-1}), $x = 0.4\%$.

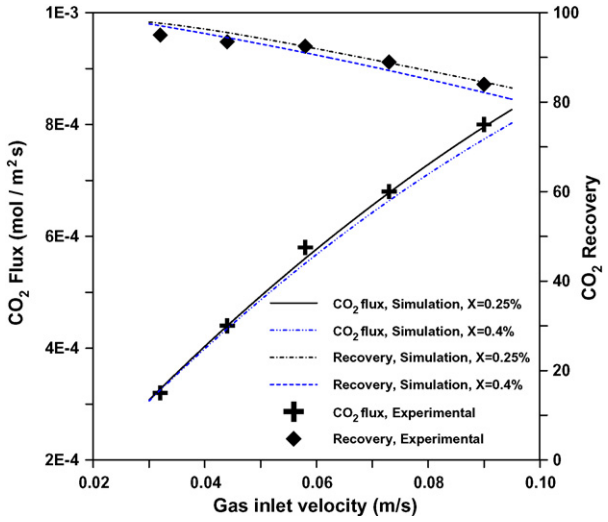

Fig. 6. CO_2 absorption flux and CO_2 recovery from a 20% CO_2–N_2 gas mixture without consideration of reactions in the liquid filled pores, $U_L = 0.12$ (m s^{-1}).

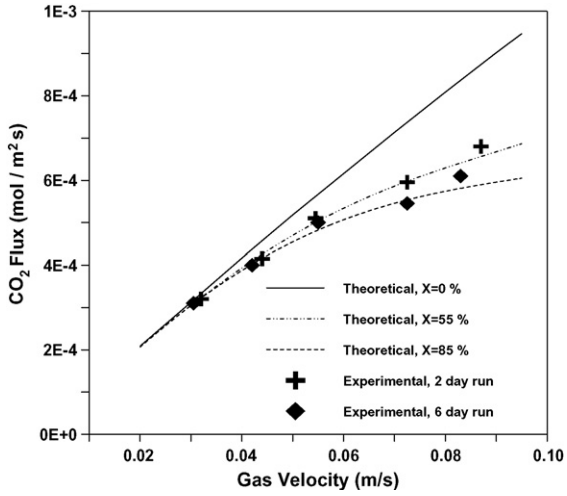

Fig. 7. CO_2 absorption flux under partial wet condition with consideration of reactions in the liquid filled pores, $U_L = 0.12$ (m s^{-1}).

reaction between CO_2 and DEA inside the wetted pores does not have significant effect in the prediction of wetting fraction. It is important to note that the negligence of chemical reaction inside the wetted pores can decrease the computer run time significantly in most cases.

As a whole the wetting fraction employed in short time analysis is very small, either with or without consideration of reactions inside the wetted pores, which indicates that the membrane wettability is week in this condition. However, as it is clear from Figs. 4 and 5, even such a small wetting can decrease the absorption flux significantly.

4.2. Long term analysis

This part refers to the long time applications of membrane module. Most of experimental and theoretical investigations on membrane contacting systems have been done very close to system start up (after steady condition) to prevent difficulties of wetting. However, it is clear that the study of long time operation of such systems is unavoidable, especially for industrial applications. Wang et al. [14] studied the performance of a polypropylene hollow fiber module over three months continuously. They found that the absorption flux decreases in the initial 4 days significantly, and there was no change in the performance afterward.

Fig. 7 presents the comparison between the proposed model and experimental data of Wang et al. [14] for second day and sixth day of module operation. In the model utilized here, the presence of chemical reactions inside the wetted pores is considered. The figure indicates that there is a good agreement between experimental data of second and sixth days run with the simulation employing wetting fractions of $x = 55$ and 85%, respectively. The wetting fraction predicted here is much higher than those of short term analysis which reveals that the membrane wetting is much more intensive in long time operations.

The model was run again to evaluate the importance of chemical reaction inside the liquid filled pores in the prediction of wetting fraction, with the assumption of no reaction in the liquid filled pores. As indicated in Fig. 8, the predicted wetting fraction in this case is $x = 0.65\%$ in sixth day, which is completely different from the result of 85% in Fig. 7. The simulation result at $x = 85\%$, which is shown in Fig. 8, with the assumption of no reaction in the liquid filled pores, has considerable difference with the experimental data. As a result, the inattention to the presence of chemical reaction in the wetted pores can produce considerable errors in the prediction of wetting fraction, even if estimated wetting fraction is small.

The two-dimensional concentration distribution of CO_2 in the liquid phase under nonwet condition, and inside the liquid phase as well as liquid filled pores under partial wet condition ($x = 85\%$) have been shown in Fig. 9a and b. As indicated in the figures, the depletion of CO_2 in radial direction is very fast near the gas–liquid interface for both nonwet and partial wet cases, although it is more intensive in nonwet situation. The variation of concentration in axial direction is stronger for nonwet case. This

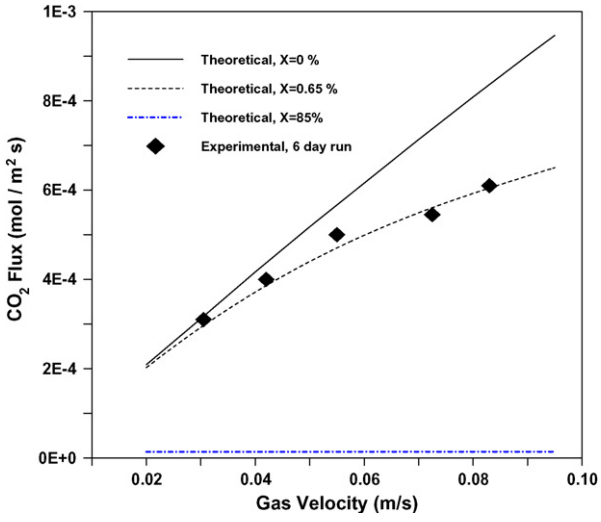

Fig. 8. CO_2 absorption flux under partial wet condition without consideration of reactions in the liquid filled pores, $U_L = 0.12$ (m s^{-1}).

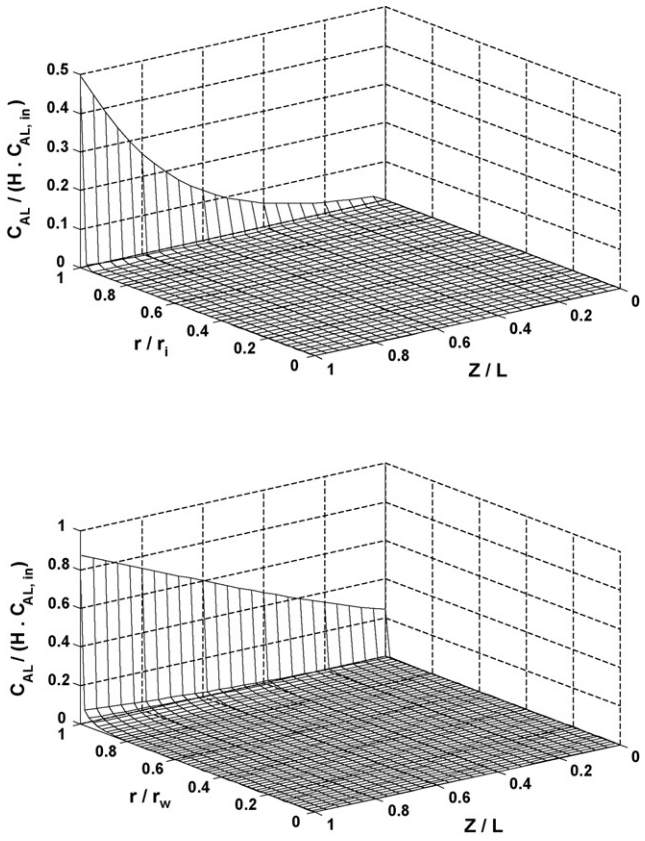

Fig. 9. Two-dimensional concentration distribution of CO_2 in the lumen and liquid filled pores, $U_L = 0.12$ (m s^{-1}), $U_g = 0.073$ (m s^{-1}). (a) CO_2 concentration distribution, $x = 0$. (b) CO_2 concentration distribution, $x = 85\%$.

is the consequence of the lower concentration of DEA available in the wetted pores in high wetting fractions, as will be discussed in the next figures.

Fig. 10 represents the two-dimensional concentration distribution of DEA for the same condition described in Fig. 9. This figure reveals a much higher variations in the concentration of DEA for partially wetted case in radial direction. The dimensionless concentration of DEA near the gas–liquid interface ($r/r_w = 1$) is as low as 0.3 for partially wetted case in comparison with 0.8 for nonwet case. This comes from the lower diffusivity of DEA in the liquid filled pores according to Eq. (15) and unavailability of convection term in Eq. (14).

The comparison of Figs. 9a and 10a (both for nonwet condition) show a very fast concentration variation of CO_2 in the gas–liquid interface, while the change in DEA concentration is relatively small. According to this result, it is possible to employ uneven grids in radial direction with smaller grid size near the gas–liquid interface and larger grid size for other parts. This method which has been used in this study and in some previous researches can decrease the computer runtime significantly by reducing number of grid points in radial direction in nonwet conditions. Unfortunately, the same approach cannot be applied in partial wet case; because according to Figs. 9b and 10b, while most of variations in CO_2 concentration is still near the gas–liquid interface, the concentration distribution of DEA is very wide in radial direction.

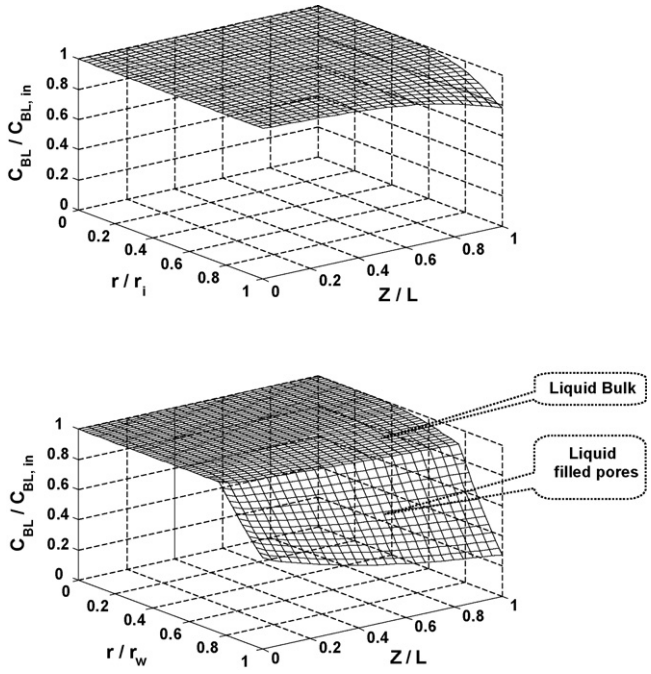

Fig. 10. Two-dimensional concentration distribution of DEA in the lumen and liquid filled pores, $U_L = 0.12$ (m s^{-1}), $U_g = 0.073$ (m s^{-1}). (a) DEA concentration distribution, $x = 0$. (b) DEA concentration distribution, $x = 85\%$.

By reconsidering Figs. 4 and 7, it is found that the wetting of membrane can decrease the absorption flux considerably, but this reduction is much more intensive in higher gas rates. This phenomenon can be described by using Figs. 10b and 11, the concentration distributions of DEA in two different gas flow rates but the same wetting fraction. It can be seen that the reduction of DEA concentration is lower in Fig. 11 (with smaller gas rate) than that in Fig. 10b (with higher gas rate). As a consequence, while the wetting fractions of two systems are the same, the higher concentration of DEA in the liquid filled pores of Fig. 11, results the more intensive reaction rate and so the lower effect of wetting in the flux reduction.

Fig. 12 presents the effect of growth of wetting fraction on the CO_2 flux, predicted by model. To have a comparison, the experimental absorption fluxes of some days are also added to

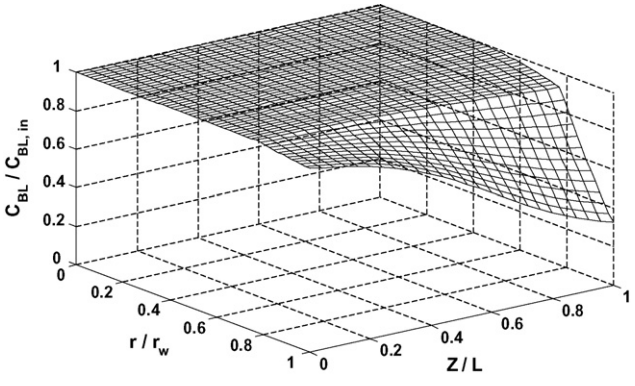

Fig. 11. Two-dimensional concentration distribution of DEA in the lumen and liquid filled pores, $U_L = 0.12$ (m s^{-1}), $U_g = 0.03$ (m s^{-1}).

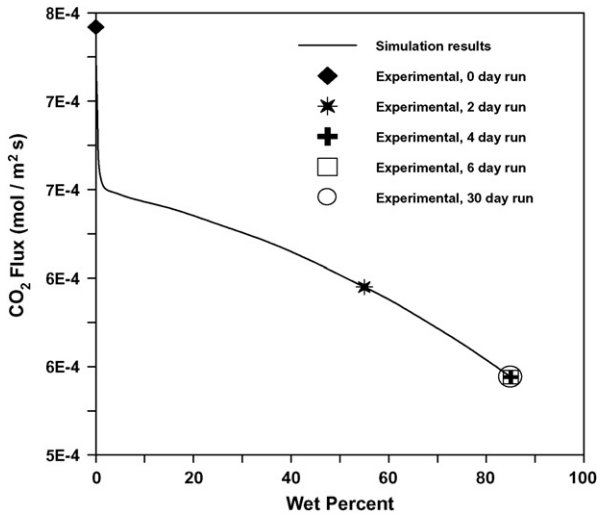

Fig. 12. The effect of wetting fraction on the absorption flux, $U_L = 0.12$ (m s^{-1}), $U_g = 0.073$ (m s^{-1}).

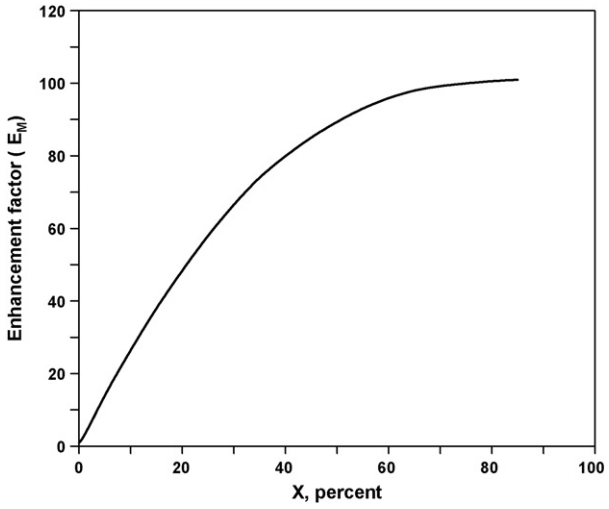

Fig. 14. The effect of wetting fraction on the chemical reaction enhancement factor, $U_L = 0.12$ (m s^{-1}), $U_g = 0.073$ (m s^{-1}).

the figure. The figure reveals that the enlargement of wetting fraction can decrease the flux significantly; however the rate of reduction is much more intensive in very low wetting fractions ($x \approx 0$–1%). A very fast reduction of flux in this small wetting fraction causes the lower CO_2 sequestration from the gas phase. It means that the concentration of CO_2 in gas phase will be increased due to wetting, which will increase the overall driving force of the system. This increase in the driving force slows down the future reduction of absorption flux. A comparison of the model prediction and experimental results shows that the wetting fraction increases from 0 to about 55% after 2 days and to 85% after 4 day; and there is no further reduction in the flux afterward.

The effect of membrane wetting on the gas phase concentration distribution is shown in Fig. 13. The figure indicates a higher concentration of CO_2 in gas phase in cases of greater wetting fraction, which is due to lower absorption flux. The increase in outlet gas concentration (at $Z/L = 0$) in cases of higher membrane wetting means that the CO_2 recovery is much lower in such cases.

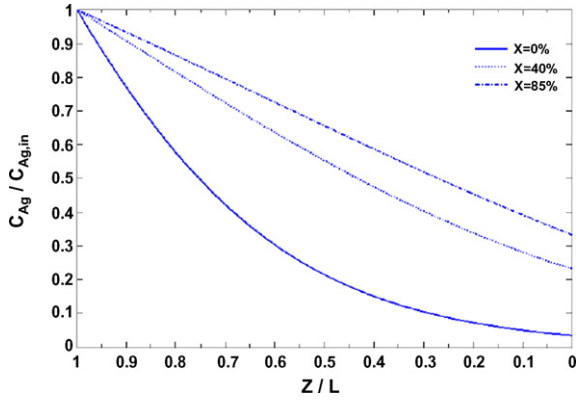

Fig. 13. Gas phase concentration distribution at different wetting fractions, $U_L = 0.12$ (m s^{-1}), $U_g = 0.073$ (m s^{-1}).

To check the importance of chemical reaction inside the liquid filled pores in more detail, Eq. (25) can be modified as:

$$\frac{1}{K_m d_{lm}} = \frac{\tau\delta(1-x)}{D_{ig_e}\varepsilon d_{lm_g}} + \frac{\tau\delta x}{D_{iL}\varepsilon d_{lm_L} H E_M} \tag{32}$$

E_M is the chemical reaction enhancement factor inside the wetted parts of the membrane. Fig. 14 shows this factor calculated by using the model and Eq. (32) versus wetting fraction of membrane. It can be seen from the figure that the value of E_M is "1" when wetting fraction is "0", but increases very fast at higher wetting fractions. This result emphasizes again that the application of Eq. (25) for the prediction of wetting fraction in presence of a chemical reaction is only valid for the cases of very small wettings.

5. Conclusion

In the present study, a mathematical model was developed for CO_2 separation by DEA solution in a hollow fiber membrane contactor operated under partially wetted condition. The developed model is able to calculate two-dimensional concentration distributions of diffusing components inside the lumen and liquid filled pores as well as axial concentration and velocity profile in the shell side, in a countercurrent flow regime. The results of the model and proposed numerical scheme show that membrane wetting, even in very low fractions, can decrease the absorption flux significantly. The analysis of concentration distribution of CO_2 and DEA under partially wetted condition shows that most of variations in CO_2 concentration are near the gas–liquid interface, while the concentration distribution of DEA is very wide in radial direction. The effect of the reversible chemical reaction between CO_2 and DEA within the liquid filled pores investigated and was found that it has considerable effect on the prediction of membrane wetting fraction.

References

[1] A. Gabelman, S.T. Hwang, Hollow fiber membrane contactors, J. Membr. Sci. 159 (1999) 61–106.

[2] J.L. Li, B.H. Chen, Review of CO_2 absorption using chemical solvents in hollow fiber membrane contactors, Sep. Purif. Technol. 41 (2005) 109–122.

[3] Q. Zhang, E.L. Cussler, Microporous hollow fibers for gas absorption. I. Mass transfer in liquid, J. Membr. Sci. 23 (1985) 321–332.

[4] Q. Zhang, E.L. Cussler, Microporous hollow fibers for gas absorption. II. Mass transfer across the membrane, J. Membr. Sci. 23 (1985) 333–345.

[5] H. Kreulen, C.A. Smolers, G.F. Versteeg, W.P.M. van Swaaij, Microporous hollow fiber membrane modules as gas–liquid contactors. Part 1. Physical mass transfer processes, a specific application: mass transfer in highly viscous liquids, J. Membr. Sci. 78 (1993) 197–216.

[6] H. Kreulen, C.A. Smolers, G.F. Versteeg, W.P.M. van Swaaij, Microporous hollow fiber membrane modules as gas–liquid contactors. Part 2. Mass transfer with chemical reaction, J. Membr. Sci. 78 (1993) 217–238.

[7] S. Karoor, K.K. Sirkar, Gas absorption studies in microporous hollow fiber membrane modules, Ind. Eng. Chem. Res. 32 (1993) 674–684.

[8] K. Li, W.K. Teo, Ues of permeation and absorption methods for CO_2 removal in hollow fiber membrane modules, Sep. Purif. Technol. 13 (1998) 79–88.

[9] K. Li, J. Kong, D. Wang, W.K. Teo, Tailor-made asymmetric PVDF hollow fibers for soluble gas removal, AIChE J. 45 (1999) 1211–1219.

[10] K. Li, J. Kong, X. Tan, Design of hollow fiber membrane modules for soluble gas removal, Chem. Eng. Sci. 55 (2000) 5579–5588.

[11] V.Y. Dindore, D.W.F. Brilman, G.F. Versteeg, Modeling of cross-flow membrane contactors: mass transfer with chemical reactions, J. Membr. Sci. 255 (2005) 275–289.

[12] R. Wang, D.F. Li, D.T. Liang, Modeling of CO_2 capture by three typical amine solutions in hollow fiber membrane contactors, Chem. Eng. Process 43 (2004) 849–856.

[13] K.A. Hoff, O. Juliussen, O.F. Pedersen, H.F. Svendsen, Modeling and experimental study of carbon dioxide absorption in aqueous alkanolamine solutions using a membrane contactor, Ind. Eng. Chem. Res. 43 (2004) 4908–4921.

[14] R. Wang, H.Y. Zhang, P.H.M. Feron, D.T. Liang, Influence of membrane wetting on CO_2 capture in microporous hollow fiber membrane contactor, Sep. Purif. Technol. 46 (2005) 33–40.

[15] H.Y. Zhang, R. Wang, D.T. Liang, J.H. Tay, Modeling and experimental study of CO_2 absorption in a hollow fiber membrane contactor, J. Membr. Sci. 297 (2006) 301–310.

[16] Y. Gong, Z. Wang, S. Wang, Experimental and simulation of CO_2 removal by mixed amines in a hollow fiber membrane module, Chem. Eng. Process 45 (2006) 652–660.

[17] H. Mahmud, A. Kumar, R.M. Narbaitz, T. Matsuura, A study of mass transfer in the membrane air-stripping process using microporous polypropylene hollow fibers, J. Membr. Sci. 179 (2000) 29–41.

[18] H. Mahmud, A. Kumar, R.M. Narbaitz, T. Matsuura, The air-phase mass transfer resistance in the lumen of a hollow fiber at low air flow, Chem. Eng. J. 97 (2004) 69–75.

[19] V.Y. Dindore, D.W.F. Brilman, F.H. Geuzebroek, G.F. Versteeg, Membrane–solvent selection for CO_2 removal using membrane gas–liquid contactors, Sep. Purif. Technol. 40 (2004) 133–145.

[20] M. Mavroudi, S.P. Kaldis, G.P. Sakellaropoulos, A study of mass transfer resistance in membrane gas–liquid contacting processes, J. Membr. Sci. 272 (2006) 103–115.

[21] V. Evren, A numerical approach to determination of mass transfer performances through partially wetted microporous membranes: transfer of oxygen to water, J. Membr. Sci. 175 (2000) 97–110.

[22] H.A. Rangwala, Absorption of carbon dioxide into aqueous solutions using hollow fiber membrane contactors, J. Membr. Sci. 112 (1996) 229–240.

[23] M. Mavroudi, S.P. Kaldis, G.P. Sakellaropoulos, Reduction of CO_2 emissions by a membrane contacting process, Fuel 82 (2003) 2153–2159.

[24] L. Bao, M.C. Trachtenberg, Modeling of CO_2-facilitated transport across a diethanolamine liquid membrane, Chem. Eng. Sci. 60 (2005) 6868–6875.

[25] P.S. Kumar, J.A. Hogendoorn, P.H.M. Feron, G.F. Versteeg, New absorption liquids for the removal of CO_2 from dilute gas streams using membrane contactors, Chem. Eng. Sci. 57 (2002) 1639–1651.

[26] S.P. Yan, M.X. Fang, W.F. Zhang, S.Y. Wang, Z.K. Xu, Z.Y. Luo, K.F. Cen, Experimental study on the separation of CO_2 from flue gas using hollow fiber membrane contactors without wetting, Fuel Process. Technol. 88 (2007) 501–511.

[27] D. deMontigny, P. Tontiwachwuthikul, A. Chakma, Using polypropylene and polytetrafluoroethylene membranes in a membrane contactor for CO_2 absorption, J. Membr. Sci. 277 (2006) 99–107.

[28] M. Caplow, kinetics of carbamate formation and breakdown, J. Am. Chem. Soc. 90 (1968) 6795–6803.

[29] P.V. Dankverts, The reaction of CO_2 with ethanolamines, Chem. Eng. Sci. 34 (1979) 443–446.

[30] P.M.M. Blauwhoff, G.F. Versteeg, W.P.M. Van Swaaij, A study on the reaction betweenCO_2 and alkanolamines in aqueous solutions, Chem. Eng. Sci. 39 (1984) 207–225.

[31] G.F. Versteeg, M.H. Oyevaar, The reaction between CO_2 and diethanolamines at 298 K, Chem. Eng. Sci. 44 (1989) 1264–1268.

[32] D.A. Glasscock, J.E. Critchfield, G.T. Rochelle, CO_2 absorption/desorption in mixtures of methyldiethanolamine with monoethanolamine or diethanolamine, Chem. Eng. Sci. 46 (1991) 2829–2845.

[33] E.B. Rinker, S.S. Ashour, O.C. Sandall, Kinetics and modeling of carbon dioxide absorption into aqueous solutions of diethanolamine, Ind. Eng. Chem. Res. 35 (1996) 1107–1114.

[34] E.B. Rinker, S.S. Ashour, O.C. Sandall, Absorption of carbon dioxide into aqueous blends of diethanolamine and methyldiethanolamine, Ind. Eng. Chem. Res. 39 (2000) 4346–4356.

[35] G. Astarita, D.W. Savage, A. Bisio, Gas Treating with Chemical Solvents, Wiley, New York, 1983.

[36] K.H. Keller, T.R.A. Stein, Two-dimensional analysis of porous membrane transport, Math. Biosci. 1 (1967) 421–437.

[37] A. Malek, K. Li, W.K. Teo, Modeling of microporous hollow fiber membrane modules operated under partially wetted conditions, Ind. Eng. Chem. Res. 36 (1997) 784–793.

[38] J. Crank, The Mathematics of Diffusion, McGraw-Hill, New York, 1967.

[39] M.C. Yang, E.L. Cussler, Designing hollow-fiber contactors, AIChE J. 32 (1986) 1910–1916.

[40] A. Constantinides, N. Mostoufi, Numerical Methods for Chemical Engineers with MATLAB Application, Prentice Hall PTR, New Jersey, 1999.

[41] R.G. Rice, D.D. Do, Applied Mathematics and Modeling for Chemical Engineers, third ed., John Wiley & Sons, New York, 1994.